Depth-related visuomotor performance in keratoconus and its relationship to stereopsis

Preetirupa Devi[1–3], Christa M. Bhengra[2], Deepak Kumar[2], Rashmi Deshmukh[4], Pravin K. Vaddavalli[4], Joshua A. Solomon[1], Christopher W. Tyler[1], & Shrikant R. Bharadwaj[1-3]

Author affiliations:

[1] Centre for Applied Vision Research, City St George's, University of London, Northampton Square, London – EC1V 0HB, UNITED KINGDOM.

[2]Brien Holden Institute of Optometry and Vision Sciences, L V Prasad Eye Institute, Road no. 2, Banjara Hills, Hyderabad – 500034, Telangana, INDIA.

[3]Prof. Brien Holden Eye Research Centre, Hyderabad Eye Research Foundation, L V Prasad Eye Institute, Road no. 2, Banjara Hills, Hyderabad – 500034, Telangana, INDIA.

[4]Shantilal Sanghvi Cornea Institute, L V Prasad Eye Institute, Road no. 2, Banjara Hills, Hyderabad – 500034, Telangana, INDIA

Corresponding author: Shrikant R. Bharadwaj

Brien Holden Institute of Optometry and Vision Sciences, L V Prasad Eye Institute, Road no. 2, Banjara Hills, Hyderabad – 500034 Telangana, INDIA.

bharadwaj@lvpei.org

Running title: Functional depth vision limitations in keratoconus

Number of figures in manuscript: 7

Number of tables in manuscript: 2

Word count in abstract: 250

Word count in revised abstract: 238

Word count in manuscript: 8163

Word count in revised manuscript: 6300

Date of submission: 23rd November 2024

Date of revised submission: 10th March 2025

Abstract

Purpose: 1) To quantify the impact of degraded binocularity in keratoconus and its improvement with rigid contact lenses on a depth-related visuomotor task that emulates complex activities in daily living; 2) to determine whether visuomotor performance may be predicted from psychophysical estimates of stereo threshold.

Methods: Participants were instructed to pass a metal loop around a wire convoluted in depth. Error rate and speed were measured in 26 controls, 30 cases with keratoconus with best-corrected spectacles, a subset of 17 cases with rigid contact lenses, and 10 uncorrected myopes with acuity and stereo thresholds comparable to the keratoconic cohort. Stereo thresholds were determined using random-dot stimuli.

Results: Binocular error rates were lower than monocular error rates for controls, uncorrected myopes, and the better-performing half of cases ($p < 0.001$, for each), but not for the worst-performing half ($p = 0.07$). Error rates in cases improved with contact lenses ($p < 0.001$). Within each cohort, the error rate was poorly correlated with the stereo threshold ($r^2 < 0.12$, for each). Monocular speeds were significantly lower than binocular speeds for controls than for cases ($p = 0.003$) and for uncorrected myopes than cases ($p = 0.001$).

Conclusions: Degraded binocularity in keratoconus may limit the ability to perform depth-related visuomotor tasks. A portion of this loss may be overcome by using rigid contact lenses. The attributes of visuomotor task performance are, however, not predictable from the psychophysical estimates of stereo thresholds.

Keywords: Blur; Contrast; Phase disruption; Retinal disparity; Visuomotor; Wavefront aberrations

`

1. Introduction

Consider the acts of inserting a key into a keyhole, placing a light bulb in its socket, or threading a needle. These seemingly straightforward activities of daily living are complex visuomotor tasks that require precise estimation of the spatial configurations for the planning and execution of appropriate hand movements and grasp actions.[1-3] The visual system's ability to estimate 3D information, particularly for motor actions as opposed to perception[3], is largely governed by the processing of retinal disparity arising from the triangulation of both eyes onto the object of interest.[4] The loss of binocularity arising from temporary occlusion or from the permanent loss of vision in one eye significantly impairs visuomotor performance.[1, 5] Similar results are observed with the deterioration of binocularity from optical blurring,[6] pathologies like amblyopia,[7, 8] and macular degeneration.[9] In general, task accuracy worsens and the speed of task performance decreases with degraded/absent depth vision, relative to viewing with intact binocularity.

This background led us to investigate the status of visuomotor task performance in the optical condition of keratoconus. This progressive ophthalmic disease, typically affecting individuals in their 2nd to 3rd decades of life,[10] is characterized by spatial and depth vision losses arising from degraded retinal image quality caused by an abnormally shaped cornea of one or both eyes.[11] The keratoconic eye's optical quality, when described using the Zernike polynomial series, shows elevated levels of coma, trefoil and spherical aberrations.[12, 13] The resultant radially asymmetric blur produces significant contrast demodulation and "doubling" or "ghosting" of local image features due to optical phase shifts.[14, 15] Usually, even in bilateral keratoconus, the grade of disease and the topography is different between the two eyes, resulting in dissimilar blur patterns.[16] The combination of the radial and bilateral asymmetry in blur significantly impacts the formation of the cyclopean image needed for processing binocularity.[14, 15] All grades of binocularity appear to be degraded in keratoconus, relative to age-similar controls: retinal disparity processing is impaired due to correspondence mismatches in the aberrated retinal images[14]; the worse of the two eyes may be suppressed,[17] and stereo thresholds maybe 3–7 fold worse, independent of keratoconus severity.[18] Motor fusion and ocular accommodation may also be impaired in keratoconus, thereby preventing clear and single binocular vision at near viewing distances.[19]

Three specific objectives surrounding the impact of the optical limitations on the depth-related visuomotor task performance in keratoconus were investigated in the present study. The primary

`

objective was to compare the monocular and binocular visuomotor task performance in keratoconic participants and similarly aged controls on a stereoscopic buzz-wire task. This task involves passing a metal loop around a wire that is convoluted in depth, avoiding contact as much as possible.[1, 5] Task performance is quantified in terms of the error rate (i.e., the frequency of contacts made between the loop and the wire per second, each of which is signalled by an audio-buzz) and the speed of loop movement along the wire. This task has been shown to reveal a greater difference between binocular and monocular viewing in controls than tasks like the peg board and bead threading because it limits the use of tactile feedback.[7, 8] We hypothesised that the degraded/absent binocularity in keratoconus would result in the error rate and speed of task performance becoming similar under monocular and binocular viewing conditions. The losses in spatial and depth vision arising from the degraded retinal image quality in keratoconus are typically managed using rigid contact lenses that replace the distorted cornea with a smoother refracting surface.[20] Therefore, the second study objective tested the hypothesis that an improvement in retinal image quality using rigid contact lenses would result in a commensurate improvement in the buzz-wire task performance in keratoconus.

While the status of binocularity may be investigated using several psychophysical paradigms, stereo thresholds obtained using dichoptic stereograms remain the most widely used measure in the clinic and in research investigations.[21] Interestingly, the depth-related visuomotor task performance of individuals with amblyopia, strabismus and in those with purposely induced degradations in binocularity have all revealed a negative correlation with their stereo threshold.[6-8] Given this, the third study objective tested the hypothesis that binocular advantages would be smaller with high stereo thresholds in keratoconus.

2. Methods

2.1. Participants

Thirty participants with keratoconus (henceforth called "cases") and 26 similarly aged participants without keratoconus (henceforth called "controls") were recruited from the patient base and staff/student pool of the L V Prasad Eye Institute (LVPEI), Hyderabad, India. An a priori power analysis was conducted using G*Power version 3.1.9.4 for sample size estimation[22], based on data from Gonzalez et al.,[23] which compared depth precision in 9 uniocular children with depth precision in 13 binocular children. The effect size in that study was 1.1, considered to be large using

`

conventional criteria.[24] With a significance criterion of α = 0.05 and power = 0.80, the minimum sample sizes needed with this effect size is N = 24 for a t-test between cases and controls, supporting the adequacy of our sample size of 30 cases and 26 controls.

The study adhered to the tenets of the Declaration of Helsinki and was approved by the Institutional Review Board of LVPEI. All participants signed a written informed consent form before study induction. Diagnosis of keratoconus was based on a comprehensive eye examination that showed evidence of keratoconus with objective, non-cycloplegic refraction, slit-lamp examination, and corneal tomography. Standard clinical management was followed for all cases, with no influence of the study protocol on their clinical care. If necessary, keratoconus was managed with rigid contact lenses as per standard operating protocols.[25] Disease severity was determined using the D-index, a multimetric measure of the corneal structural deformation, obtained using Scheimpflug imaging tomography (Pentacam HR®, Oculus Optikgeräte; Wetzlar, Germany).[26] The D-index was derived for both eyes of all participants using the Belin-Ambrósio enhanced ectasia display map and included deviations of front and back surface elevations of the cornea, pachymetric progression, thinnest corneal point, and deviation of Ambrósio relational thickness maximum.[26] This metric has been shown to have good reliability in the diagnosis and progression of keratoconus, with higher D-index values indicating greater disease severity.[27]

The best spectacle-corrected, high contrast, monocular distance visual acuity in each eye, as estimated using the routine clinical protocol, ranged from 0.00 to 1.60 logMAR in cases. The equivalent acuity values were all 0.00 logMAR in controls (20/20; visual acuity beyond 0.00 logMAR is typically not measured in the clinical protocol at the institute where the study is conducted). All cases and controls had monocular near acuities between 0.00 and 0.40 logMAR (N8) at 40 cm. Unaided visual acuity was not recorded in this study. Participants with any other ophthalmic dysfunction, or any systemic condition that resulted in restricted body movement, visible shaking of hands, inability to follow instructions, or inability to fuse the stereogram for stereopsis measurements, were excluded.

Seventeen cases were habitual rigid contact lens users [one case wore a Rose K2® lens (Menicon Co. Ltd., Nagoya, Japan), while the rest wore conventional rigid gas permeable lenses (Purecon McAsfeer, Silver line laboratory Pvt. Ltd, India)] (*Appendix 1*). Based on the severity and requirement

`

for contact lenses, 11 participants wore contact lenses in both eyes and the rest wore these lenses only in one eye (*Appendix 1*). The lenses were fitted by experienced contact lens practitioners at LVPEI, using the manufacturers' recommended protocols, and the final lenses were ordered and dispensed to the participants as a part of regular clinical protocol. The visual acuity, stereo thresholds and the buzz-wire performance were tested both before and after contact lens fitting. The visual acuities ranged from 0.00 to 0.40 logMAR with their contact correction.

2.2. The buzz-wire apparatus and task performance

The buzz-wire apparatus and task have been described in detail by Devi et al.[5] Briefly, the apparatus comprised of a 33.5 cm long wire of 1 mm diameter shaped into three horizontal depth curves, with its edges clamped onto vertical posts (Figure 1A). The wire pattern was mounted parallel to the horizontal plane, resulting in continuous changes in depth from one end to the other (free-fuse the stereo pair in Figure 1B to experience the depth impression). A 10 mm diameter metal loop, held by hand with a 9 cm long stalk, was guided along the wire and delivered an auditory buzz each time the loop came in contact with the wire (Figure 1A). Three buzz-wire apparatuses with similar amounts of depth modulation but different wire patterns due to slight phase shifts were employed in this study to assess task reproducibility. Devi et al.[5] determined that, if the wire were to be at the center of the loop in the buzz-wire task, the gap between the wire and one end of the loop would subtend a mean diastereopsis disparity of 611 arcsec (range: 450 - 715 arcsec, depending on the participant's interpupillary and viewing distances) (see Figure 7 in Devi et al).[5] The entire apparatus, the participants' face, and the experimental surrounding were video recorded using the front camera of a standard cellular phone (Redmi Note 5 Pro®, Xiaomi, China) that was fixed to a custom-built clamp at 30 cm from the buzz-wire apparatus (field of view captured by the phone camera: 42° x 55°).

Participants were positioned 30 cm away from the buzz-wire at an average elevation angle of ~45° (inter-participant range depending on their height: 36 - 53°) (Figure 1A), so that it provided both monocular and stereoscopic cues to its convolutional structure. The buzz-wire task was described as a "game" to the participants, with the following instructions given at the beginning of the game, verbatim in English or in their local language:

> "Look at the camera without moving for 5 seconds, during which I will give a verbal countdown and say START, upon which you will start the game. Your task is to pass the loop from one end to

the other end without touching the wire. In case, the loop touches the wire, you will hear the buzzer ring. When you hear the buzzer, stop your movement, and make the buzzing stop by centring the wire within the circular loop. Once the buzzing stops, proceed forward until you reach the other end. Make sure the loop is held upright throughout the game".

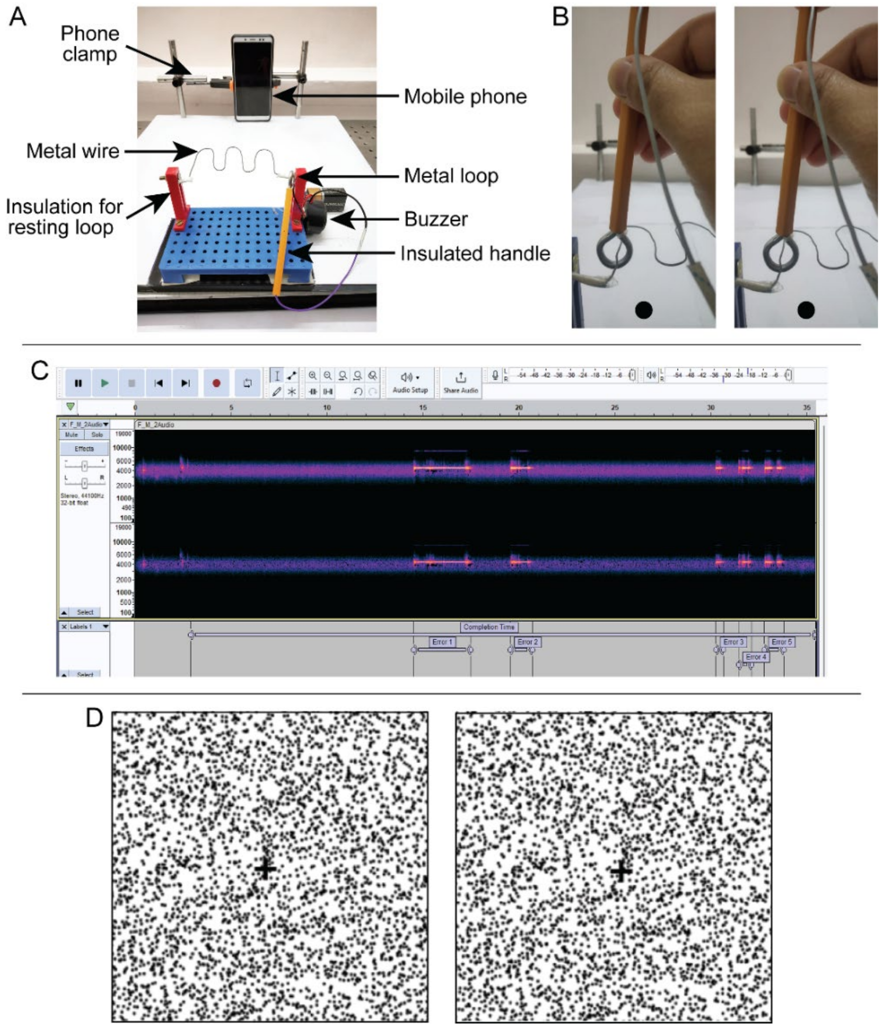

Figure 1: *Panel A) The buzz-wire apparatus from the participant's viewpoint with the key elements highlighted. Panel B) A representative, stereoscopic photograph depicting the position of the metal loop around the wire track. Readers can cross-fuse the two images to view the pattern in 3D. Panel C) A representative spectrogram used for the audio analysis of the buzzes using the Audacity® software. The spectrogram shows the labels marked for the completion time and for the epochs of error time stamps (high contrast tracks in the spectrogram) during a representative trial. Panel D) A representative, cross-fusible, example of the random-dot stereogram used for estimating the stereo threshold. The fused stereogram shows a leftward tilted rectangular bar in crossed retinal disparity.*

No explicit instructions were provided to the participants on the speed with which they needed to play the game. The instructions were reiterated at the beginning of each experimental trial. The instructions were accompanied by the examiner demonstrating each step to ensure the participants

`

understood what should and should not be done.[28, 29] However, no prior practice trials were given to the participants to retain the difference in the viewing conditions.[7] The direction of movement of the loop, i.e., from the left end to the right end of the wire or vice versa — was randomized at the beginning of each trial. All participants performed the buzz-wire task under binocular and monocular viewing conditions. They performed the task thrice for each viewing condition with different patterns of the wire formation, all in random order. For monocular viewing of controls, one eye was randomly occluded, while the worse eye (based on visual acuity) of cases was occluded to minimize the impact of resolution loss on task performance. In cases with equal acuity in both eyes, one eye was randomly occluded. Their heads remained free to move during the task. Each run took approximately 40 sec to complete, following which participants were given 1-min of break prior to the next trial.

The trial began once it was ensured that the participant was looking straight at the camera in the apparatus (Figure 1A). The task performance in each trial was recorded for offline analysis. After task completion, the examiner manually checked every video to discard trials where the participant dragged the loop along the wire, a strategy deemed invalid for task completion. The accepted video files were then analysed using custom-written software in Python (3.10 Version, Centrum voor Wiskunde en Informatica Amsterdam, The Netherlands). The videos were first cropped from the beginning of the task to its end, as determined by the examiner's verbal utterance of the word START to the metal loop entering the insulated portion of the wire on the other end. The videos were then analysed for buzzes using the open-source Audacity® software (3.2.1 version, Audio.com, Boston, USA) (Figure 1C). The spectrogram of the audio signal generated by the movement of the loop along the wire, including the buzzes, was then bandpass filtered to a frequency range of 4 to 4.1 kHz. Intensities outside this frequency range were cut off at –30 dB to differentiate buzzes from the background noise (Figure 1C). The total number of buzzes and the time stamps corresponding to the onset and termination of each buzz were then computed for the entire video.

2.3. Estimation of outcome variables from the buzz-wire task

The elapsed time between the beginning and end of the video file was deemed as the total task duration (in seconds). Error rate was calculated as the frequency of occurrence of the error buzzes over the total task duration (in errors/sec). The speed at which the task was completed, when the participant was not making an error, was calculated as the length of the wire (33.5 cm) divided by

`

the error-free time (in cm/sec). The error-free time, in turn, was calculated as the total task duration minus the total time spent in making the errors (each error epoch was defined as the elapsed time between the start and end of the error buzz). The binocular advantage in error rate was calculated as the ratio of the monocular to binocular error rate (in case of zero error rate, the respective values were arbitrarily replaced by 0.001, as described in Devi et al.[5]). Similarly, the binocular advantage in speed was calculated as the ratio of binocular to monocular speed. In both cases, a ratio greater than unity indicated superior performance under binocular than monocular viewing.

2.4. Measurement of stereo threshold

Stereo threshold was measured at a 50 cm viewing distance using random-dot stimuli presented on a gamma calibrated LCD monitor (1680 × 1050 pixel resolution, 59 Hz refresh rate) and controlled using the Psychtoolbox-3 interface of MATLAB (R2016a; The MathWorks, Natick, USA).[30] The random-dot stimuli incorporated a rectangular disparity-defined bar oriented either with a leftward or a rightward tilt in crossed retinal disparity (Figure 1D). The dichoptic stimuli were fused using a handheld stereo viewer with built-in periscopic mirrors to adjust for the participant's horizontal phoria and interpupillary distance (Screen-Vu Stereoscope, Portland, USA). Vertical phoria, if any, was corrected with minor adjustments in head orientation. Data collection began once the participant reported stable fusion of the bounding box that presented the random-dot stimuli (Figure 1D). Participants identified the direction of the bar tilt for every stimulus presentation while the retinal disparity varied in a 2 down and 1 up adaptive staircase manner with each presentation. For a better visibility of the stereoscopic rectangular bar, the initial disparity value was set anywhere between 2000 and 4000 arcsec. Until the first reversal, the disparity was changed by 50% of the previous disparity value. At the subsequent reversals, the disparity changed with a 5% step size. The staircase was terminated after 11 reversals. Response frequencies were fit with Weibull functions to obtain maximum-likelihood estimates and credible intervals for the 70.7% correct threshold level.[31]

2.5. Protocol

The buzz-wire and stereo tasks were performed by all participants with natural pupils and accommodative states. Among the cases, the first measurements were always made with their habitual spherocylindrical spectacles and then with their habitual rigid contact lenses, if any. The measurements were made in this order so as to not to deform the cornea with the rigid contact lens wear, which, in turn, would alter the pattern of retinal image blur experienced by the participant.[32] Change in the monocular task performance with contact lens wear was not determined in this study.

2.6. Schematic framework for data interpretation

To enable ease of interpretation, the data clouds obtained for error rate and speed in controls and cases were fit with bivariate contour ellipses using plot_ellipse.m code in Matlab.[33] The x- and y-coordinates of the centroid and the major axes of the ellipses were determined from the fits. These outcomes were interpreted in the context of a schematic framework described below (Figure 2A). In this schematic, the binocular and monocular error rates are plotted against each other. Whereas the 45° line of equality indicates no binocular advantage and thus dominance of the task by monocular factors (purple cloud in Figure 2A), data below this line would indicate a performance advantage derived from binocular depth cues (e.g. retinal disparity) and/or from the integration of monocular cues (e.g., occlusion, perspective cues) from the two eyes. The data could be uniformly distributed below the line of equality, indicating a uniform binocular advantage across the range of monocular error rates (blue cloud in Figure 2A). The orientation of the data could also be steeper than 45°, indicating that the binocular and monocular error rates are becoming more and more similar, with an increase in the monocular error rates (turquoise cloud in Figure 2A). That is, the binocular advantage in error rate reduces with an increase in the monocular error. This could indicate that the binocular advantage in error rates may be determined by factors that limit the monocular performance in this task (e.g., retinal image quality, in this case) or simply that the error rates have reached the maximum that could be measured by the apparatus.

A range of possible comparisons between controls and cases is further illustrated in Figures 2B - I. The data of cases and controls may overlap along the line of equality, indicating no impact of viewing condition or cohort on task performance (Figure 2B). The data clouds may remain overlapped but with both shifted below the line of equality, indicating a significant impact of only viewing condition but not cohort on task performance (Figure 2C). The data clouds may also appear translated along the equality line, indicating a significant impact of cohort (cases producing more errors than controls in this schematic) but not of viewing condition on task performance (Figure 2D). The data clouds may be shifted below the line of equality and appear horizontally translated relative to each other, indicating significant impact of both viewing condition and cohort but with no interaction between the factors (Figure 2E). Figures 2F–I show data clouds wherein the main effect of both factors and the interaction between them are significant. In Figure 2F, the binocular advantage is present only for controls and not for cases. In Figures 2G and H, the binocular advantage is present for both cohorts, but only one cohort shows a monocular dependence of the binocular advantage - cases in Figure 2G and controls in Figure 2H. Finally, in Figure 2I the binocular advantage in error rates show monocular dependence, but to varying extents, in both cohorts. This data schematics can also be extrapolated to the speed of task performance wherein faster movement under binocular viewing is indicated by the data lying above the line of equality (schematic not shown here).

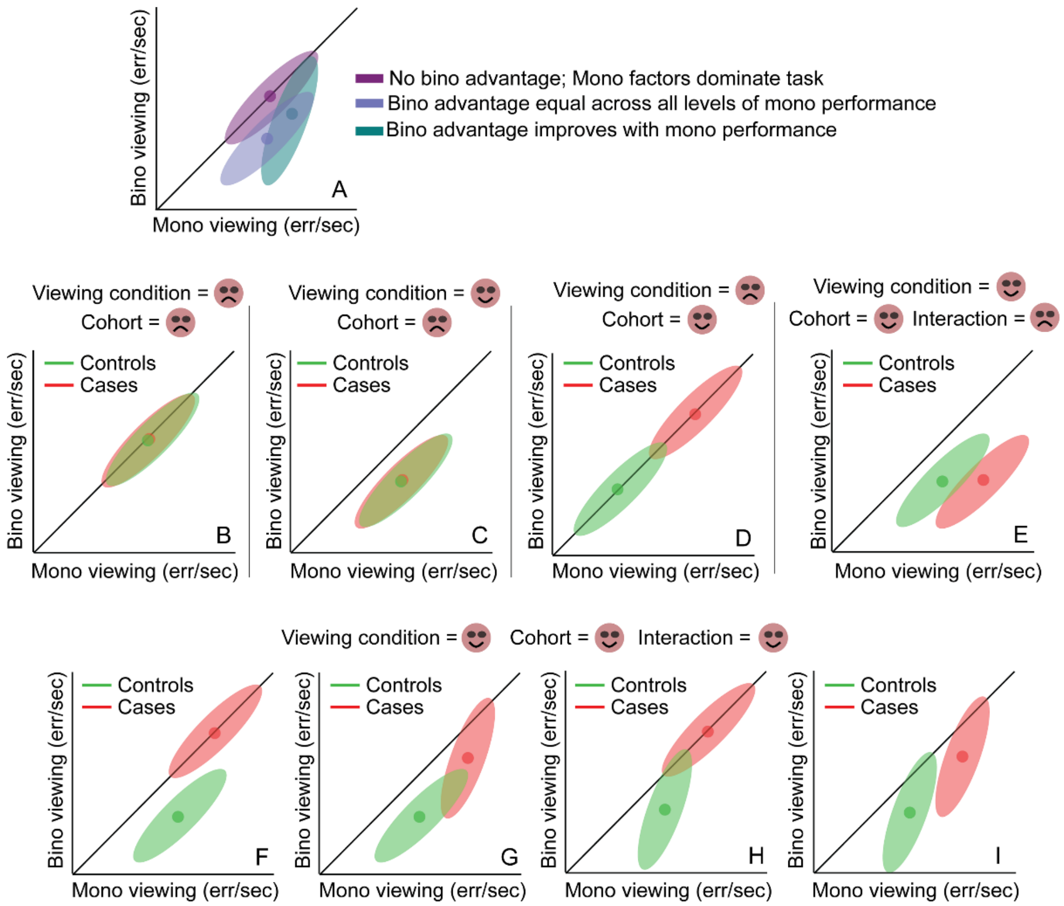

Figure 2: *Schematics for the different pattern of results that may be obtained across controls and cases for the error rates in the buzz-wire task used in this study. Data clouds are assumed to have elliptical distributions. The solid circle is the centroid of the elliptical data cloud. The "smiley" face indicates statistically significant impact of the independent variable (i.e., viewing condition) on the dependent variable (i.e., error rate, in this case) while the "gloomy" face* indicates no evidence of such a statistical significance. Panels B–I are described in the text.

2.7. Data analyses

Statistical analyses were performed using IBM SPSS Statistics® (Version 21; Armonk, NY), Matlab (R2016a) and Wolfram Mathematica (Version 14.1.0, Wolfram Research, Inc., Champaign, IL). Since there were no overall trends in the error rate or speed across the three repetitions of the buzz-wire task,[5] these quantities were averaged for further analyses. The Shapiro-Wilk test revealed that error rate, speed and the binocular advantage of error rate and speed were non-normally distributed. Hence, the datasets of error rate and speed were Box-Cox transformed using a λ value of 0.15 and the datasets of binocular advantage of error rate and speed were log transformed to achieve normality, thereby making them amenable to parametric statistics. Note, however, that Figures 3 - 6 containing the study results are all constructed on the raw untransformed data for visualization purposes. Two-factor repeated measures multiple analysis of variable (RM-MANOVA) was performed to investigate the between-subject factor of cohort type (controls vs. cases) and the within-subject factor of viewing condition (binocular vs. monocular) on the dependent variables of error rate and speed. A separate one-factor, between-subjects MANOVA was performed to compare the binocular advantage in error rate and speed between controls and cases. Similarly, a separate one-factor, within-subjects MANOVA was performed to compare the impact of optical correction modality (rigid contact lens vs. spectacles) on stereo threshold, error rate, and speed.

2.8. Comparison of buzz-wire performance in cases with those of uncorrected myopes

The results from the main experiment revealed that the monocular and binocular buzz-wire task performance was worse in cases than in controls. An additional experiment was performed to determine whether this deterioration was unique to keratoconus or generic to any form of optical blur experienced by the individual – for instance, optical blur from uncorrected axial myopia, but with a regularly shaped cornea. This experiment tested the hypothesis that the error rate and speed in the buzz-wire task will be similar in cases and uncorrected myopic cohorts with comparable levels of visual acuity and stereo thresholds. Ten participants with –6.00D to –13.00D of uncorrected myopia (21 - 34 years) repeated the monocular and binocular versions of the buzz-wire task. All other details were identical to the main experiment.

3. Results

Table 1 describes the demographic and clinical details of the study participants *(see Appendix 1 for individual cases)*. Ten of the 30 cases had bilateral keratoconus with similar severity in both eyes. The remaining were either bilateral keratoconus with different disease severities in the two eyes or those with a clinically manifest keratoconus in only one eye (Appendix 1).

3.1. Buzz-wire task performance in controls and cases

Figure 3A shows scatter diagrams of the binocular and monocular error rate for controls and cases with their habitual spectacles. The error rate patterns in both cohorts resembled the schematic in

Table 1: *Demographic and clinical details of study participants*

<table>
<tr><td rowspan="9">Cases (n = 30)</td><td>Age (years)</td><td colspan="2">20 (17 to 34)</td></tr>
<tr><td>Sex (M : F)</td><td colspan="2">20 : 10</td></tr>
<tr><td></td><td>Right eye</td><td>Left eye</td></tr>
<tr><td>D-index (unitless)</td><td>8.09 (2.13 to 27.13)</td><td>7.28 (0.53 to 22.05)</td></tr>
<tr><td>SER (D)</td><td>–3.50 (–12.00 to 0.00)</td><td>–3.50 (–24.00 to –0.38)</td></tr>
<tr><td>J_0 (D)</td><td>0.00 (–2.59 to 2.82)</td><td>0.09 (–2.35 to 4.59)</td></tr>
<tr><td>J_{45} (D)</td><td>0.77 (–0.94 to2.95)</td><td>–0.99 (–3.87 to 2.38)</td></tr>
<tr><td>BSCVA (logMAR)</td><td>0.30 (0.00 to 1.60)</td><td>0.30 (0.00 to 1.40)</td></tr>
<tr><td>Stereo threshold (arcsec)</td><td colspan="2">547.13 (52.66 to 1906.00)</td></tr>
<tr><td rowspan="9">Controls (n = 26)</td><td>Age (yrs)</td><td colspan="2">24 (17 to 29)</td></tr>
<tr><td>Sex (M : F)</td><td colspan="2">10 : 17</td></tr>
<tr><td></td><td>Right eye</td><td>Left eye</td></tr>
<tr><td>D-index (unitless)</td><td>0.72 (–0.37 to 2.45)</td><td>0.76 (–1.16 to 2.61)</td></tr>
<tr><td>SER (D)</td><td>0.00 (–5.00 to 0.88)</td><td>0.00 (–5.00 to 0.88)</td></tr>
<tr><td>J_0 (D)</td><td>0.00 (0.00 to 1.25)</td><td>0.00 (0.00 to 1.25)</td></tr>
<tr><td>J_{45} (D)</td><td>0.00 (0.00 to 0.00)</td><td>0.00 (0.00 to 0.32)</td></tr>
<tr><td>BSCVA (logMAR)</td><td>0.00 (0.00 to 0.00)</td><td>0.00 (0.00 to 0.00)</td></tr>
<tr><td>Stereo threshold (arcsec)</td><td colspan="2">29.99 (3.18 to 77.70)</td></tr>
</table>

The values indicate the median (minimum to maximum) for each parameter described in the study. The SER, J_0 and J_{45} power vector terms represent the spherical equivalent of refraction and the regular and oblique astigmatic components of refraction, respectively.[34] BSCVA = best spectacle-corrected visual acuity.

Figure 2G. The orientation and the centroid locations of the bivariate contour ellipse for controls indicated a uniform shift in the data below the line of equality (Figure 3A). In contrast, the bivariate contour ellipse for cases was steeper than 45°, with its y-axis centroid remaining significantly lower than its x-axis centroid (Figure 3A). Additionally, the rightward and upward shift in the x and y-axes centroids, respectively, of cases, relative to controls, indicated an overall higher error rates in cases than in controls (Figure 3A).

The bivariate contour ellipses for speed were oriented close to the 45° line of equality in controls and cases (Figure 3B). For controls, the x-axis centroid of the ellipse was lower than the y-axis centroid, indicating a slowing down under monocular viewing condition (Figure 3B) while in cases, the x- and y-axes centroids for cases were not different to each other (Figure 3B), indicating that the cases did not slow down as much as the controls under monocular viewing. Additionally, the speed ellipse of cases was shifted rightwards, relative to controls, suggesting that under monocular viewing, the former cohort performed the task faster than the latter cohort under monocular viewing conditions (Figure 3B).

The Box-Cox transformed monocular error rates of controls and cases were higher than the binocular values (Table 2, Section 1a). The multivariate test in the two-factor RM-MANOVA revealed significant main effects of viewing condition and cohort and significant interaction between the two main effects on the combined dependent variables of error rate and speed (Table 2, Section 2a). These effects were retained in the univariate tests, with the effect size being stronger for the former

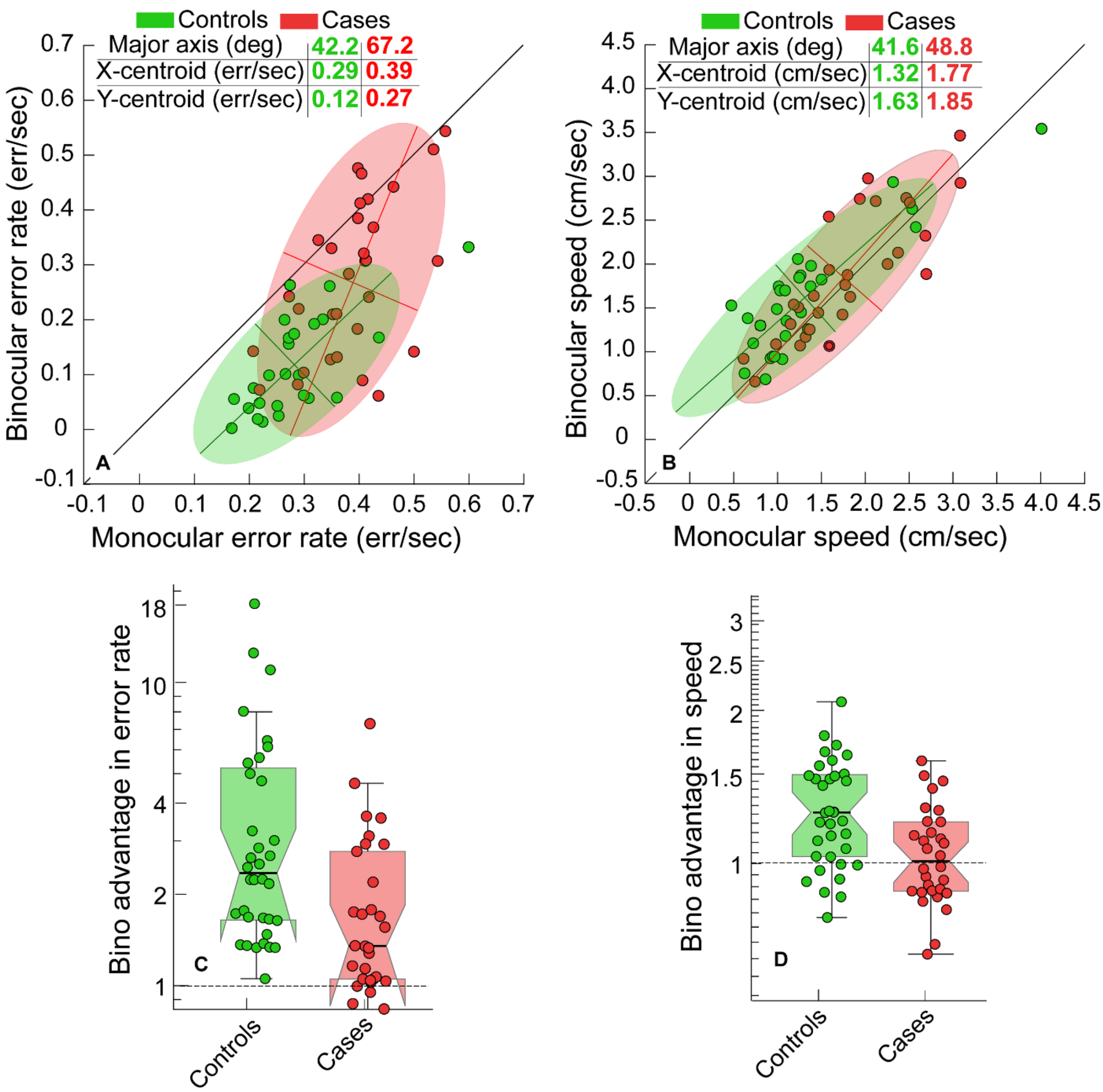

Figure 3: *Scatter diagrams of the error rate (panel A) and speed (panel B) obtained from controls (green symbols) and cases (red symbols) while performing the buzz-wire task in this study. The coloured patches represent the best-fit bivariate contour ellipse for the controls and cases datasets. The major and minor axes are shown for each ellipse, the intersection of which represents its centroid. The diagonal line in each panel represents the line of equality for monocular and binocular performance. The gestalt obtained from these contours may be readily compared with the schematics described in Figure 2. Panels C and D show the Box and Whisker plots of the binocular advantage in error rate and speed obtained for controls and cases in this study, respectively. For each box and whisker plot, the horizontal line is the median, the edges are the 25th and 75th quartiles and the whiskers are the 1st and 99th quartiles. The green and the red dots are the individual data points, jittered randomly along the X-axis for ease of visualization.*

Table 2: *Results of the main statistical analyses conducted in this study.*

Section 1: T-Tests

1a. Paired t-tests

			Error rate			Speed		
			Mean diff ± SEM	**t value**	**p-value**	**Mean diff ± SEM**	**t value**	**p-value**
Comparison of error rate and speed among controls and cases	Control	Bino vs Mono	−1.00 ± 0.19	−5.23	**<0.001**	0.26 ± 0.06	4.26	**<0.001**
	KC	Bino vs Mono	−0.44 ± 0.09	−4.92	**<0.001**	0.03 ± 0.05	0.5	0.62
	KC below threshold	Bino vs Mono	0.71 ± 0.10	−7.11	**<0.001**	–		
	KC above threshold	Bino vs Mono	0.08 ± 0.04	−1.93	0.07			

Section 2: Two-factor RM-MANOVA Analysis

Effect of viewing condition (Bino vs Mono) and cohort type (control vs cases) on error rate and speed

2a. Multivariate tests

	F	**p-value**	**Partial η^2**
Viewing condition	41.8	**<0.001**	0.61
Cohort type	9.33	**<0.001**	0.26
Viewing condition x Cohort type	11.72	**<0.001**	0.31

2b. Univariate tests

		Error rate			Speed		
		Mean ± SEM	**p-value**	**Partial η^2**	**Mean ± SEM**	**p-value**	**Partial η^2**
Viewing condition	Binocular	−1.73 ± 0.11	**<0.001**	0.48	0.50 ± 0.06	**<0.001**	0.24
	Monocular	−1.03 ± 0.03			0.36 ± 0.06		
Cohort type	Controls	−1.66 ± 0.10	**<0.001**	0.26	0.31 ± 0.08	**0.03**	0.08
	KC	−1.10 ± 0.10			0.55 ± 0.08		
Viewing condition x Cohort type	–	–	**0.004**	0.15	–	**0.004**	0.14

Section 3: One-factor RM-MANOVA Analysis

Binocular advantage in error rate and speed among control and cases

3a. Multivariate tests

	F	**p-value**	**Partial η^2**
Cohort type	13.06	**< 0.001**	0.33

3b. Univariate tests

		Error rate			Speed		
		Mean ± SEM	**p-value**	**Partial η^2**	**Mean ± SEM**	**p-value**	**Partial η^2**
Cohort type	Controls	0.53 ± 0.06	**< 0.001**	0.21	0.14 ± 0.03	**0.003**	0.13
	KC	0.22 ± 0.06			0.02 ± 0.03		

Section 4: One-factor MANOVA Analysis

Effect of spectacle and contact lenses on stereo, error rate and speed

4a. Multivariate tests

	F	**p-value**	**Partial η^2**
Correction modality	163.89	**<0.001**	0.97

4b. Univariate tests

		Stereo threshold		Error rate		Speed	
		Mean ± SEM	**p-value**	**Mean ± SEM**	**p-value**	**Mean ± SEM**	**p-value**
Correction modality	Spectacle	2.71 ± 0.12	**0.001**	−1.23 ± 0.12	**<0.001**	0.69 ± 0.12	**0.001**
	Contact lens	2.34 ± 0.12		0.76 ± 0.02		1.10 ± 0.01	

Section 5: One-factor RM-MANOVA Analysis

Effect of viewing on error rate and speed among uncorrected myopes

5a. Multivariate tests

	F	**p-value**	**Partial η^2**
Viewing condition	23.06	**0.001**	0.72

5b. Univariate tests

		Error rate			Speed		
		Mean ± SEM	**p-value**	**Partial η^2**	**Mean ± SEM**	**p-value**	**Partial η^2**
Viewing condition	Binocular	−1.56 ± 0.12	**0.001**	0.72	0.16 ± .15	**0.003**	0.64
	Monocular	−0.99 ± 0.05			0.08 ± 0.19		

Section 6: Mann-Whitney test

			Error rate			Speed		
			Median (IQR)	**Z**	**p-value**	**Median (IQR)**	**Z**	**p-value**
Bino advantage myopes Vs. cases with comparable stereo loss	Cohort type	Myopes	1.98 (1.37 – 2.32)	−2.26	**0.02**	1.27 (1.09 – 1.53)	−2.72	**0.005**
		Cases	1.16 (0.99 – 1.81)			1.03 (0.87 – 1.12)		

Section 1 shows the results of t-tests comparing the binocular vs. monocular performances of controls and cases. Sections 2a and b show the results of the multivariate and univariate two-factor RM-MANOVA comparing the binocular and monocular task performances of controls and cases, respectively. Section 3a and b show the results of the multivariate and univariate one-factor RM-MANOVA comparing the binocular advantages for the two outcome variables in controls and cases. Sections 4a and b show the results of the multivariate and univariate one-factor MANOVA comparing the impacts of correction modality on the stereoacuity and error rate of cases. Sections 5a and b show the results of the multivariate and univariate one-factor MANOVA reporting the impacts of viewing condition on the error rate and speed in uncorrected myopes. Section 6 shows the results of the Mann-Whitney test comparing the binocular advantages in error rates and speed among uncorrected myopes and cases with comparable stereo loss. ***The*** *mean ± standard error of the mean (SEM) shown here are the Box-Cox transformed values, as described in the Methods section. The mean values shown here may be retransformed to its raw form by using the formula:* $x_{raw} = \sqrt[\lambda]{\lambda\, x_{trans} + 1}$, *where* x_{raw} *is the mean of the raw data,* x_{trans} *is the mean of the transformed data, and* λ *is the Box-Cox transformation exponent used in this study (*$\lambda = 0.15$*). Relationships with* $p < 0.05$ *(uncorrected for multiple comparisons) appear in bold.*

than the latter outcome variable (Table 2, Section 2b). To further investigate the pattern of error rates obtained in cases, their monocular and binocular error rates were divided into two subgroups about the y-axis centroid i.e., participants with binocular error rates lower and higher than the y-axis centroid. The mean difference in the Box-Cox transformed monocular and binocular error rates was found to be significant only for the latter subgroup and not the former subgroup (Table 2, Section 1a).

The one-factor MANOVA performed on the log-transformed binocular advantage scores showed a significant difference between controls and cases for the combined dependent variables (Figure 3C and D, Table 2, Section 3a). The univariate tests showed that the binocular advantages in error rate and speed were higher in controls than in cases, with the effect size being higher for error rate than speed (Table 2, Section 3b). These trends were expected from the binocular and monocular data of these outcome variables reported in Table 2, Sections 1 and 2.

3.2. Relationship between stereo threshold and binocular advantage in error rate

Unlike controls, the addition of binocularity had a differential impact on error rates of cases (Figure 3A). To determine if this pattern was related to the participants' stereo thresholds, the binocular advantages in error rates of cases were plotted against their stereo thresholds (Figure 4). The same relationship for controls is also shown in this figure for comparison. All controls had stereo thresholds lower than the buzz-wire task's diastereopsis threshold (vertical line in Figure 4), making the task a suprathreshold activity. While all the controls showed a distinct binocular advantage in error rate, this advantage was poorly correlated with stereo threshold (Pearson's $r = -0.25$, $p = 0.22$).

Only 10 cases had stereo thresholds lower than the diastereopsis threshold, all of whom also showed a binocular advantage in the error rate (Figure 4). Amongst the remaining 20 cases with stereo thresholds poorer than the diastereopsis disparity threshold, 10 exhibited near unity binocular advantage, 3 had binocular advantage comparable to that of controls and the binocular advantage of the rest was somewhere in between (Figure 4). Overall, like controls, there was a non-significant correlation between binocular advantage in error rate and stereo threshold in the cases (Pearson's r = –0.32, p = 0.08).

Amongst cases, binocular advantage in error rate poorly correlated with the two eyes' maximum D-index, the difference between the two eyes' D-indices, and the maximum, mean, and the difference between the two eyes' best-corrected visual acuity (r ≤ –0.32, p ≥ 0.08, for all).

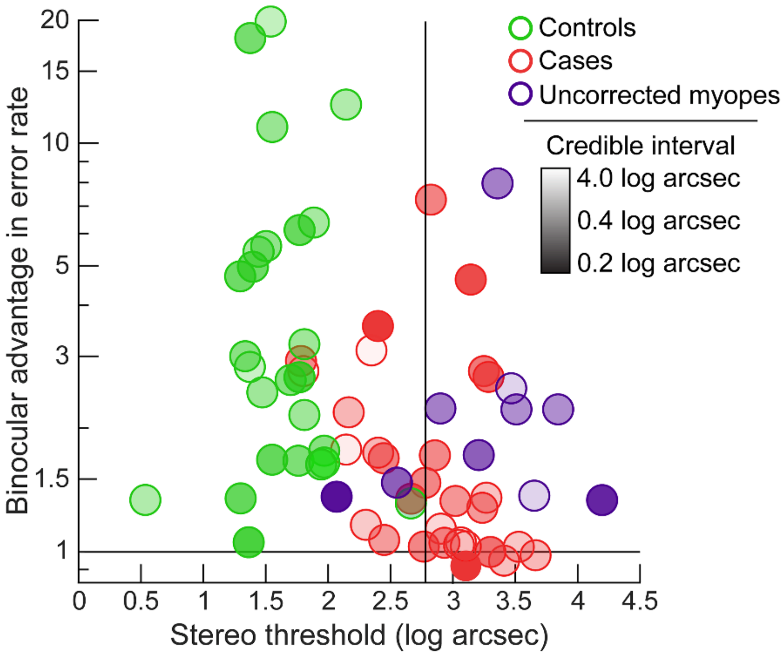

Figure 4: *Binocular advantage in error rate plotted against the random-dot stereo threshold for controls (green), cases (red), and uncorrected myopes (blue). The transparency of the dots represents the 68% credible interval for the stereo thresholds. The vertical line indicates the disparity threshold (611 arcsec or 2.79 log arcsec) for diastereopsis.*[5, 23] *The horizontal line denotes the level where there was no binocular advantage.*

3.3. Impact of rigid contact lenses on the error rates of the cases

With rigid contact lens wear, the stereo threshold and error rate of cases were below the 1:1 line, indicating an improvement in these variables relative to spectacles (Figure 5A and B, Table 2, Section 4b). The one-factor MANOVA showed a statistically significant impact of the correction modality for the combined dependent variables (Table 2, Section 4a). The univariate tests confirmed this effect for both stereo threshold and error rate, with the effect size being larger for the latter than the former variable (Table 2, Section 4b). However, the proportional improvements in stereo threshold and error rate, obtained by dividing the value obtained with spectacles by the value obtained with contact lenses, proved to be uncorrelated (Pearson's r = 0.02, p = 0.94; Figure 5C).

3.5. Buzz-wire task performance of uncorrected myopes

Visual acuities amongst the uncorrected myopes (0.91 ± 0.07 logMAR) were significantly poorer than amongst those cases that were above the diastereopsis threshold (0.50 ± 0.07 logMAR; t = 4.01, p = 0.001). Stereo thresholds, on the other hand, were comparable between the two cohorts (uncorrected myopes: 3.28 ± 0.20 log arcsec; cases: 3.20 ± 0.06 log arcsec, t = 0.43, p = 0.67) (blue vs red bubbles in Figure 4)].

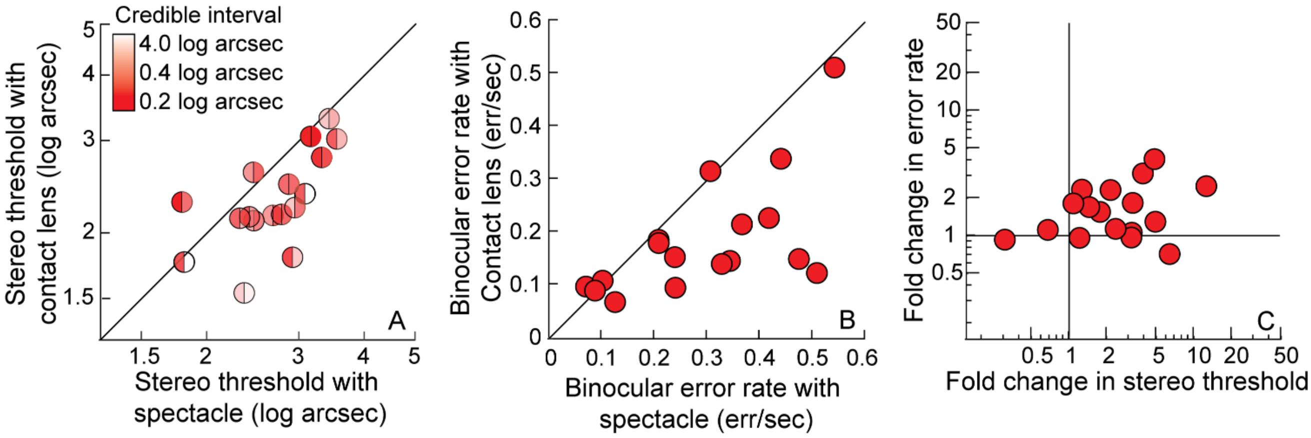

Figure 5: *Panels A and B show the stereo threshold and error rate, respectively, obtained with the spectacle and contact lens corrections in cases. The transparency on the right and left hemispheres in Panel A, represents the 68% credible interval for the spectacle and contact lens, respectively. Panel C shows the fold-change in stereo threshold from spectacles to contact lens wear plotted against the corresponding fold-change in error rates of the buzz-wire task. The region above the intersection of the vertical and horizontal lines indicates an improvement in both parameters with contact lens wear in this panel. The region diagonally opposite this indicates worsening of performance in both parameters with contact lens wear.*

Scatter diagrams of error rate and speed for the participants with uncorrected myopia have been fit with bivariate contour ellipses and superimposed on the corresponding ellipses for controls and cases in Figure 6. The bivariate contour ellipse for error rates in the uncorrected myopes was oriented at 57.9°, with its x-axis centroid remaining higher than its y-centroid (Figure 6A). The one-factor RM-MANOVA analysis showed a significant impact of viewing condition on the combined dependent variable (Table 2, Section 5a) and the univariate tests confirmed a significant impact of viewing condition for both error rates and speed (Table 2, Section 5b). The log-transformed binocular advantage in error rate (mean ± SEM: 0.22 ± 0.04) was well correlated with logMAR visual acuity (Pearson's r = –0.73; p = 0.02) (data not shown) but poorly correlated with stereo threshold

(Pearson's r = –0.09; p = 0.80) (Figure 4). The binocular advantages in error rate and speed were also significantly higher amongst uncorrected myopes than amongst cases with comparable levels of stereo threshold (Figure 4; Table 2, Section 6).

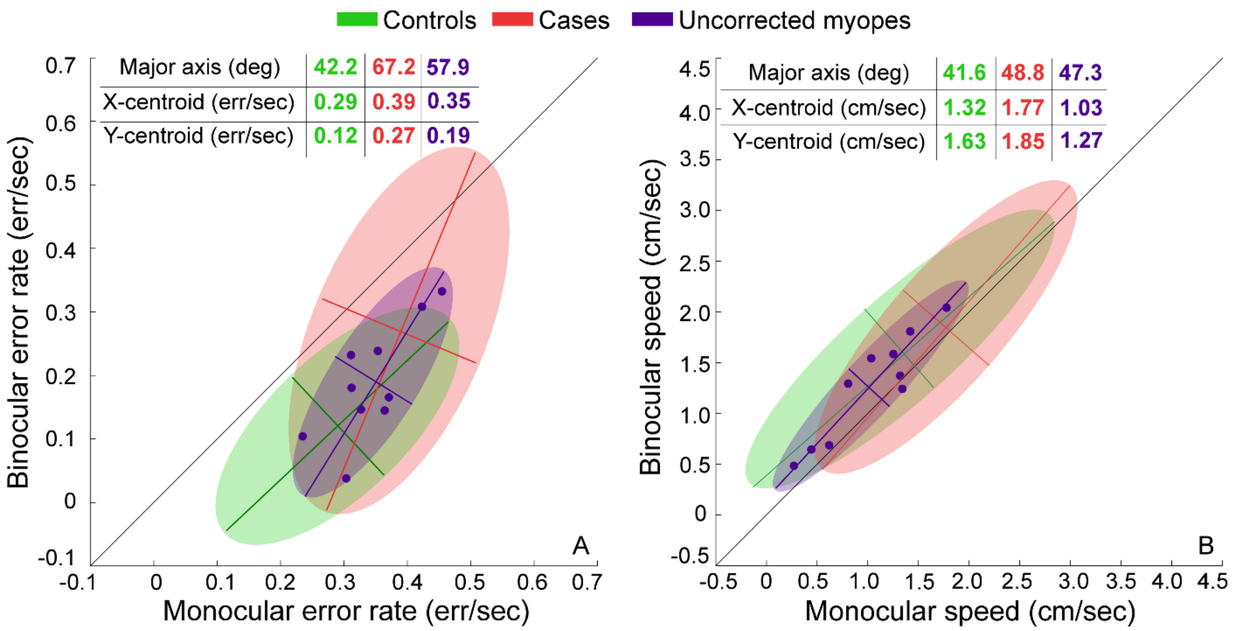

Figure 6: *Scatter diagrams of the error rate (panel A) and speed (panel B) in uncorrected myopes (blue symbols) while performing the buzz-wire task plotted along the corresponding bivariate contour ellipses. The ellipses of the controls (green) and cases (red), identical to those in Figure 3, are also reproduced here for comparison purposes. All other details are the same as Figure 3.*

4. Discussion

4.1. Summary of results

1. Controls made fewer errors when viewing the buzz wire binocularly (Table 2, Figure 3A). However, only those cases with relatively low monocular error rates showed a similar advantage from binocular viewing (Figure 3A). Cases with high monocular error rates also had higher error rates when viewing the buzz wire binocularly (Table 2, Figure 3A).
2. An improvement in the retinal image quality of cases with rigid contact lens wear reduced the binocular error rates in the buzz-wire task, vis-à-vis, spectacles (Figure 5B).
3. Two observations indicate that psychophysical estimates of stereo thresholds may not be a good predictor of error rates in visuomotor activities like the buzz-wire task. First, stereo threshold proved to be poorly correlated with the binocular advantage in error rate amongst the participants within each cohort. Second, stereo threshold proved to be poorly correlated with the reduction in error rate enjoyed by cases, when they switched from their best-corrected spectacles to contact lenses (Figure 5C).

4. Controls, uncorrected myopes and cases executed the buzz-wire task faster under binocular than monocular conditions (Figures 3B and 6B). However, the magnitude of speed reduction from binocular to monocular viewing was smaller in cases than in the controls and uncorrected myopes (Figures 3B and 6B, Table 2).

These results compare well with previous findings of deficient visuomotor task performance in other forms of ophthalmic disease such as amblyopia and strabismus[7, 8], and indicates that functional depth vision may be severely compromised with degraded binocularity, irrespective of the cause of this dysfunction. Finally, these results also align well with those of Knill, who showed that visuomotor tasks like hand reaching are heavily weighted towards the binocular retinal disparity cue, with little influence of monocular cues on task performance.[3]

4.2. Stereo threshold as poor predictor of visuomotor task performance

There are at least two reasons why the psychophysical stereo threshold may correlate poorly with error rate in the buzz-wire task. First, the executive requirements of the random-dot stereogram task and the buzz-wire task may be quite different.[35] The former is a hyperacuity task, requiring good quality correspondence matching of the monocular images for fusion, computation of retinal disparity from the fused percept, and an inference about the geometric shape of the 3D object in an otherwise two-dimensional field of random dots.[36] The buzz-wire task, on the other hand, relies on accurate and continuous judgment of the diastereopsis of a physical 3D structure that guides hand movements to avoid contact between the loop and the wire in the task.[5] These two measures may respond very differently to the degraded retinal image quality experienced in the present study. Random-dot stereo targets may be more vulnerable to the contrast loss and phase distortions in the blurred retinal image,[15, 37] reaching stereo-blindness levels when thresholds exceed 1300 arc sec,[38] while useful information regarding diastereopsis may still be available in the buzz-wire task for comparable levels of blur. Evidence for this possibility arises from the uncorrected myopes continuing to show a binocular advantage in the buzz-wire task, even while they were all nearly stereo-blind (Figures 4 and 6A). This binocular advantage may be derived from non-stereoscopic cues that may aid the identification of the gap between the loop and the wire in this task, unlike random-dot stereograms that are entirely reliant on the retinal disparity cue for stereo processing. However, the prominent monocular cue of motion parallax derived from head movements may not be useful for depth judgments in the buzz-wire task, as reported recently by Devi et al.[5] The

`

complexity of integrating retinal image motion arising from head velocity with the velocity of object motion arising from passing the loop through the buzz wire may make this cue less beneficial to the present task performance.[5]

The second reason is that the stereoscopic information in a random-dot target is to be inferred from a two-dimensional field of random dots might make this task more unnatural and, thus, more vulnerable to retinal image quality degradation. On the contrary, the buzz-wire task is similar to routine depth-related activities of daily living wherein the stereoscopic information is derived from objects that are physically separated in space. Perhaps a top-down knowledge of the buzz-wire configuration, and/or the depth information derived from convergence eye movements while tracking the depth convoluted buzz-wire makes this task less vulnerable to retinal image quality degradation.[39] After all, our ability to generate accurate vergence eye movements remains largely unaffected in the presence of either iso-ametropic or anisometropic retinal image blur.[40] Future studies could employ depth judgments between physically separated objects to determine the relationship between stereo thresholds and errors in the buzz-wire task.

4.3. Retinal image quality and its impact on visuomotor task performance

The nature of blur experienced by the participant and its bilateral (a)symmetry could have a determining impact on the buzz-wire task investigated in this study. Deeper insights into this issue may be obtained through simulation of how the buzz-wire apparatus may appear from the blur in cases, uncorrected myopia, and in controls (Figure 7). All the following simulations were performed for 555 nm light and 5 mm pupil diameter, using standard Fourier optics techniques.[41] The point spread function (PSF) of the eye with clear vision was generated using only population average higher-order Zernike wavefront aberrations obtained from Cheng et al.[42] (Figure 7A). The PSFs of uncorrected myopes were generated by adding 1 D, 3 D, and 10 D worth of defocus to the population average higher-order Zernike aberrations (Figures 7B - D, respectively). Case PSFs are obtained from higher-order Zernike aberrations, corresponding to early, mild, moderate and severe keratoconus already available in the laboratory (Figures 7E–H).[12] Lower-order aberrations are assumed to be fully corrected in keratoconus, while in reality, some may remain owing to variability in estimating the subjective refraction endpoint.[43, 44]

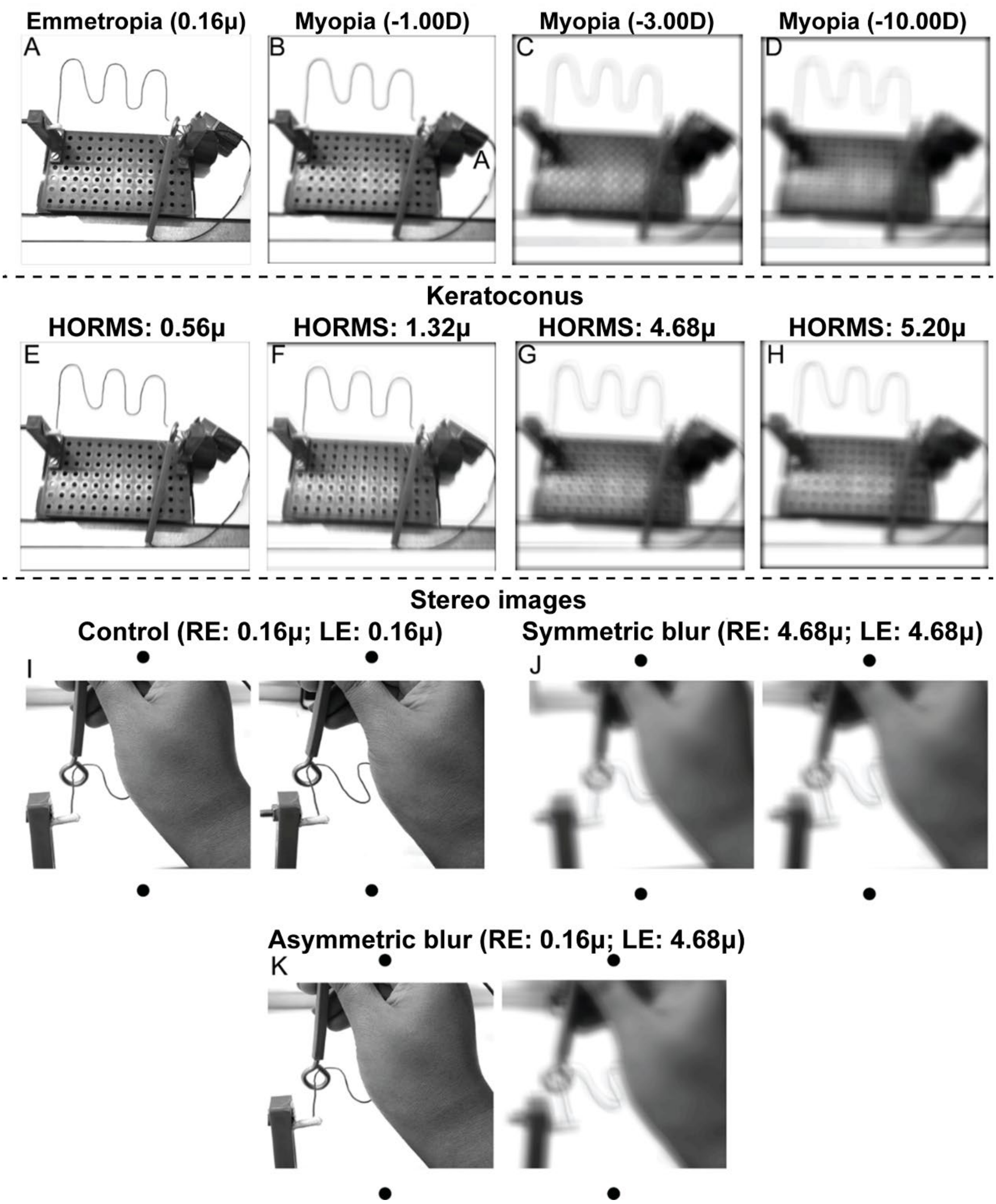

Figure 7: *Panels A–H) Point-of-view optical simulations of the buzz-wire apparatus with clear vision (panel A), blurred vision from uncorrected myopia (panels B – D) and blurred vision from cases, whose severity is indicated on top of each panel by the root-mean-squared values of the higher-order aberrations (HORMS) (panels E–H). Panels I–K show* cross-fusible *zoomed-in stereoscopic image pairs of the buzz-wire apparatus illustrating the location of the loop relative to the wire when vision is clear in both eyes (panel I) and when vision is bilaterally (panel J) or unilaterally (panel K) blurred from keratoconus. The wavefront aberration values used to blur the right eye (RE) and left eye (LE) of the stereogram are indicated in each figure panel.*

The uncorrected myopes in the present study were all iso-ametropic, resulting in similar magnitudes of radially symmetric blur in the two eyes. This radial symmetric blur is characterized largely by contrast demodulations while retaining the spatial relationship between the loop and the wire (Figures 7B–D). The bilateral symmetry of blur continues to support the fusion of the monocular percept (Figure 7J). Both features may help retain the diastereopsis information under binocular viewing in uncorrected myopia (Figure 7J). In contrast, the cases experience radially *asymmetric* blur that may be of bilaterally dissimilar owing to interocular differences in disease severity (Table A1). The radially asymmetric blur introduces significant phase distortions that disrupt the spatial relationship between the loop and the wire under monocular viewing (manifesting as "ghosting" or "doubling" of the wire in Figures 7E–H).[15] Binocularly, the phase distortions may disrupt the correspondence matching between the monocular precepts[14] and the bilaterally asymmetric blur may induce interocular suppression of the more blurred percept,[17] both of which may lead to poor quality diastereopsis (Figure 7K). These effects may explain the absence of binocular advantage in the buzz-wire task for the cases, even while it was retained in the uncorrected myopes (Figure 6). Relative to spectacles, rigid contact lenses may have improved buzz-wire task performance in cases by reducing the contrast demodulation and phase disruption in the monocular retinal images and by improving the symmetry in the retinal image quality of the two eyes.[15, 17, 37] A future study could compare the buzz-wire task performance in uncorrected anisometropia and bilaterally asymmetric keratoconus to gain deeper insights into this issue. The improved error rates in the buzz-wire task of cases with rigid contact lenses could also be a learning effect, as the buzz-wire task was first performed with spectacles and then with contact lenses. However, Devi et al.[5] investigated this possibility and found no evidence of a learning effect over the three trials. Nonetheless, future studies may systematically investigate the impact of any learning effect on the buzz-wire task performance.

4.4. Clinical implications

The present results suggest that keratoconus may increase the difficulty in executing activities of daily living that involve 3D depth judgments (e.g., driving, navigating obstacles and climbing stairs) (Figure 3). These factors, combined with their sub-optimal spatial vision,[11] may contribute towards an overall deterioration in their quality of life and general well-being.[45] Rigid contact lenses that improve retinal image quality may be one way to minimize this deterioration (Figure 5B). Interestingly, neither the disease severity nor the routinely evaluated clinical measures of visual acuity or stereoacuity were good predictors of such visuomotor activity limitations (Figure 4). This observation, on one hand, reveals the limitation of the clinical measures in reflecting the real-world visual experience of the patient, and, on the other hand, underlines the need for expanding the visual assessment battery to include measures that emulate the complexities of daily tasks.

`

The lack of a prominent speed reduction in the buzz-wire task in keratoconus is contrary to the expectation of how this parameter may decline in the presence of uncertain sensory inputs (arising from blurred vision and poor stereopsis, in this case[11, 18]). This may be so for two reasons. First, the binocular and monocular viewing experience in keratoconus in such tasks may be similar, given their habitually sub-optimal vision. Thus, there may be no overt reason to decrease the speed under monocular viewing, relative to binocular viewing. Second, keratoconics may harbour false beliefs that they can see well in depth despite their degraded binocularity. This may reflect the general personality trait of keratoconics and the difficulties they may experience coping with vision loss.[46, 47] These hypotheses need further investigation.

5. Acknowledgements

The authors thank all the volunteers that participated in this study. The study was financially support through the Hyderabad Eye Research Foundation, L V Prasad Eye Institute. Dr Shrikant Bharadwaj was supported by a Fulbright–Nehru Academic and Professional Excellence Fellowship offered by the United States India Education Foundation (USIEF) during the writing phase of this manuscript.

6. References

1. Read JC, Begum SF, McDonald A, Trowbridge J. The binocular advantage in visuomotor tasks involving tools. *Iperception* 2013;4:101-110.
2. Fielder AR, Moseley MJ. Does stereopsis matter in humans? *Eye (Lond)* 1996;10:233-238.
3. Knill DC. Reaching for visual cues to depth: the brain combines depth cues differently for motor control and perception. *Journal of Vision* 2005;5:103-115.
4. Wheatstone C. On some remarkable and hitherto unobserved phenomena of binocular vision. *Phil Trans Roy Soc, London* 1838;128:371-394.
5. Devi P, Solomon JA, Tyler CW, Dave TV, Kaliki S, Bharadwaj SR. Comparison of depth-related visuomotor task performance in uniocular individuals and in binocular controls with and without temporary monocular occlusion. *Invest Ophthalmol Vis Sci* 2024;65:32.
6. Piano ME, O'Connor AR. The effect of degrading binocular single vision on fine visuomotor skill task performance. *Invest Ophthalmol Vis Sci* 2013;54:8204-8213.
7. O'Connor AR, Birch EE, Anderson S, Draper H. Relationship between binocular vision, visual acuity, and fine motor skills. *Optom Vis Sci* 2010;87:942-947.
8. O'Connor AR, Birch EE, Anderson S, Draper H, Group F. The functional significance of stereopsis. *Invest Ophthalmol Vis Sci* 2010;51:2019-2023.
9. Verghese P, Tyson TL, Ghahghaei S, Fletcher DC. Depth perception and grasp in central field loss. *Invest Ophthalmol Vis Sci* 2016;57:1476-1487.
10. Santodomingo-Rubido J, Carracedo G, Suzaki A, Villa-Collar C, Vincent SJ, Wolffsohn JS. Keratoconus: An updated review. *Cont Lens Anterior Eye* 2022;45:101559.
11. Kumar P, Campbell P, Vaddavalli PK, Hull CC, Bharadwaj SR. Structure-function relationship in keratoconus: Spatial and depth Vision. *Transl Vis Sci Technol* 2023;12:21.
12. Nilagiri VK, Metlapally S, Schor CM, Bharadwaj SR. A computational analysis of retinal image quality in eyes with keratoconus. *Sci Rep* 2020;10:1321.

13. Pantanelli S, MacRae S, Jeong TM, Yoon G. Characterizing the wave aberration in eyes with keratoconus or penetrating keratoplasty using a high-dynamic range wavefront sensor. *Ophthalmology* 2007;114:2013-2021.
14. Metlapally S, Bharadwaj SR, Roorda A, Nilagiri VK, Yu TT, Schor CM. Binocular cross-correlation analyses of the effects of high-order aberrations on the stereoacuity of eyes with keratoconus. *J Vis* 2019;19:12.
15. Marella BL, Conway ML, Vaddavalli PK, Suttle CM, Bharadwaj SR. Optical phase nullification partially restores visual and stereo acuity lost to simulated blur from higher-order wavefront aberrations of keratoconic eyes. *Vision Res* 2024;224:108486.
16. Ferdi AC, Nguyen V, Gore DM, Allan BD, Rozema JJ, Watson SL. Keratoconus natural progression: A systematic review and meta-analysis of 11 529 eyes. *Ophthalmology* 2019;126:935-945.
17. Marella BL, Conway ML, Suttle C, Bharadwaj SR. Contrast rivalry paradigm reveals suppression of monocular input in keratoconus. *Invest Ophthalmol Vis Sci* 2021;62:15.
18. Nilagiri VK, Metlapally S, Kalaiselvan P, Schor CM, Bharadwaj SR. LogMAR and stereoacuity in keratoconus corrected with spectacles and rigid gas-permeable contact lenses. *Optom Vis Sci* 2018;95:391-398.
19. Dandapani SA, Padmanabhan P, Hussaindeen JR. Spectrum of binocular vision anomalies in keratoconus subjects. *Optom Vis Sci* 2020;97:424-428.
20. Deshmukh R, Ong ZZ, Rampat R, et al. Management of keratoconus: an updated review. *Front Med (Lausanne)* 2023;10:1212314.
21. Scheiman M, Wick B. *Clinical management of binocular vision: heterophoric, accommodative, and eye movement disorders*: Lippincott Williams & Wilkins; 2008.
22. Faul F, Erdfelder E, Lang A-G, Buchner AJBrm. G* Power 3: A flexible statistical power analysis program for the social, behavioral, and biomedical sciences. 2007;39:175-191.
23. Gonzalez E, Steinbach M, Ono H, Wolf M. Depth perception in children enucleated at an early age. *Clinical Vision Sciences* 1989;4:173-177.
24. Cohen J. *Statistical power analysis for the behavioral sciences*. 2 ed: Hillsdale, NJ: Lawrence Erlbaum Associates, Publishers; 1988.
25. Downie LE, Lindsay RG. Contact lens management of keratoconus. *Clin Exp Optom* 2015;98:299-311.
26. Hashemi H, Beiranvand A, Yekta A, Maleki A, Yazdani N, Khabazkhoob M. Pentacam top indices for diagnosing subclinical and definite keratoconus. *J Curr Ophthalmol* 2016;28:21-26.
27. Muftuoglu O, Ayar O, Hurmeric V, Orucoglu F, Kilic I. Comparison of multimetric D index with keratometric, pachymetric, and posterior elevation parameters in diagnosing subclinical keratoconus in fellow eyes of asymmetric keratoconus patients. *J Cataract Refract Surg* 2015;41:557-565.
28. Granados-Delgado P, Casares-Lopez M, Martino F, Anera RG, Castro-Torres JJ. The Role of Visual Performance in Fine Motor Skills. *Life (Basel)* 2024;14.
29. Hou SW, Zhang Y, Christian L, Niechwiej-Szwedo E, Giaschi D. Evaluating visuomotor coordination in children with amblyopia. *Dev Psychobiol* 2022;64:e22270.
30. Brainard DH. The Psychophysics Toolbox. *Spat Vis* 1997;10:433-436.
31. Watson AB. Probability summation over time. *Vision Res* 1979;19:515-522.
32. Jinabhai A, O'Donnell C, Radhakrishnan H. Changes in refraction, ocular aberrations, and corneal structure after suspending rigid gas-permeable contact lens wear in keratoconus. *Cornea* 2012;31:500-508.
33. Gillay Z. Plot ellipse on scattered 2D data. *https://inmathworkscom/matlabcentral/fileexchange/116610-plot-ellipse-on-scattered-2d-data Accessed on 10 Sept 2024* 25 Aug 2022.
34. Thibos LN, Wheeler W, Horner D. Power vectors: an application of Fourier analysis to the description and statistical analysis of refractive error. *Optom Vis Sci* 1997;74:367-375.
35. Stevenson SB, Cormack LK, Schor CM. Hyperacuity, superresolution and gap resolution in human stereopsis. *Vision Res* 1989;29:1597-1605.
36. Julesz B. Binocular depth perception of computer-generated patterns. *Bell System Technical Journal* 1960;39:1125-1162.
37. Marella BL, Vaddavalli PK, Reddy JC, Conway ML, Suttle CM, Bharadwaj SR. Interocular contrast balancing partially improves stereoacuity in keratoconus. *Optom Vis Sci* 2023;100:239-247.

`

38. Chopin A, Bavelier D, Levi DM. The prevalence and diagnosis of 'stereoblindness' in adults less than 60 years of age: a best evidence synthesis. *Ophthalmic Physiol Opt* 2019;39:66-85.
39. Rogers B. When is a disparity not a disparity? Toward an old theory of three-dimensional vision. *Iperception* 2023;14:20416695231202726.
40. Bharadwaj SR, Candy TR. Accommodative and vergence responses to conflicting blur and disparity stimuli during development. *J Vis* 2009;9:4 1-18.
41. Jaskulski M TL, Bradley A, Kollbaum P. IRIS – Indiana Retinal Image Simulator. 2019.
42. Cheng H, Barnett JK, Vilupuru AS, et al. A population study on changes in wave aberrations with accommodation. *J Vis* 2004;4:272-280.
43. Davis LJ, Schechtman KB, Begley CG, Shin JA, Zadnik K. Repeatability of refraction and corrected visual acuity in keratoconus. The CLEK Study Group. Collaborative Longitudinal Evaluation of Keratoconus. *Optom Vis Sci* 1998;75:887-896.
44. Raasch TW, Schechtman KB, Davis LJ, Zadnik K, Study CSGCLEoK. Repeatability of subjective refraction in myopic and keratoconic subjects: results of vector analysis. *Ophthalmic Physiol Opt* 2001;21:376-383.
45. Gothwal VK, Gujar R, Sharma S, Begum N, Pesudovs K. Factors affecting quality of life in keratoconus. *Ophthalmic Physiol Opt* 2022;42:986-997.
46. Aiello F, Gallo Afflitto G, Ceccarelli F, et al. Keratoconus and personality traits: A case-control study. *Cornea* 2024;43:237-244.
47. Mannis MJ, Ling JJ, Kyrillos R, Barnett M. Keratoconus and personality-A Review. *Cornea* 2018;37:400-404.

Appendix

Table A1: *Demographic details of the 30 keratoconic participants along with their corneal topographic outcomes (maximum keratometry and D–index) and visual functions (logMAR visual acuity and stereo thresholds) with spectacles and contact lens.*

Sub No.	Age (yrs)	Sex	Maximum Keratometry *(D)*		D–index *(unitless)*		Visual acuity with spectacles *(logMAR)*		Stereo threshold with spectacles (arc sec)	Visual acuity with contact lens *(logMAR)*		Stereo threshold with contact lens (arc sec)
			RE	LE	RE	LE	RE	LE		RE	LE	
1	19	M	45.5	70.8	2.96	16.77	0.00	0.60	841.97	*	0.10	820.65
2	18	M	44.6	79.3	2.13	22.05	0.00	1.10	3372.25	*	0.40	1032.86
3	19	M	55.5	44.1	8.06	0.53	1.40	0.00	800.18	0.00	0.00	62.03
4	19	M	58.5	51.4	7.97	5.51	0.30	0.18	462.70	0.30	0.00	142.78
5	22	M	56.7	48.8	7.94	4.29	0.40	0.00	222.54	0.18	0.00	33.94
6	22	F	67.6	50.7	14.2	6.44	0.70	0.00	1159.30	0.00	*	233.76
7	20	F	44.9	43.0	9.41	4.12	0.18	0.00	63.31	0.10	0.00	56.88
8	25	M	56.6	57.0	7.19	7.89	0.00	0.30	281.38	*	0.00	127.48
9	26	F	48.6	55	3.87	6.89	0.00	0.10	60.62	0.00	0.00	192.58
10	17	M	60.1	52.6	11.09	5.89	0.30	0.18	278.80	0.00	0.00	401.12
11	26	F	61.3	57.1	14.96	16.32	0.30	0.18	584.58	0.00	0.00	145.83
12	32	M	48.5	64.6	7.27	12.8	0.18	0.48	251.90	*	0.00	138.43
13	18	M	62.4	75.5	8.38	16.95	0.18	0.30	1390.05	0.00	0.00	1115.27
14	21	F	53.6	41.4	10.12	3.36	0.70	0.10	1997.88	0.00	*	601.26
15	18	M	56.8	49.8	11.96	6.83	0.40	0.18	855.42	0.00	0.00	169.57
16	24	M	56.1	61.9	9.03	8.7	0.00	0.40	717.63	0.10	0.00	296.03
17	24	M	49.7	50	6.99	6.52	0.18	0.10	200.85	0.00	0.10	134.62
18	25	F	54.4	52.7	4.85	4.63	0.18	0.18	666.34	NA	NA	NA
19	17	M	48.5	55.6	3.38	7.67	0.30	0.30	1855.71	NA	NA	NA
20	34	F	53.2	53.1	4.99	3.58	0.30	0.30	1773.45	NA	NA	NA
21	22	M	63.6	60.2	11.29	10.2	0.18	0.10	146.20	NA	NA	NA
22	28	M	52.9	42.8	5.31	1.35	0.48	0.48	250.76	NA	NA	NA
23	19	M	63.3	55.2	14.44	8.33	0.48	0.18	601.53	NA	NA	NA
24	22	M	44	46	2.27	5.17	0.30	0.18	139.60	NA	NA	NA

25	19	F	65.9	44.6	NA	4	1.10	0.00	4596.21	NA	NA	NA
26	24	F	71.3	50.8	24.6	16.3	0.90	0.18	1118.56	NA	NA	NA
27	20	M	62.4	53.5	11.67	11.24	0.60	0.48	1720.88	NA	NA	NA
28	18	M	62.4	52.5	27.13	10.17	1.60	0.80	1269.90	NA	NA	NA
29	28	F	46.9	54.4	8.09	10.71	0.30	0.40	1927.61	NA	NA	NA
30	17	M	48.9	52.3	9.89	12.49	0.70	1.10	1048.99	NA	NA	NA

Abbreviations: max K: maximum keratometry reading, stereo: stereo threshold, RE: right eye, LE: left eye, SP: spectacle, CL: contact lens, *NA: not applicable (these participants were not tested with contact lens correction). Participants 1 – 17 performed the task with both spectacles and contact lenses. The asterisk symbol indicates participants wore contact lens only in one eye, for which the visual acuity is reported. The fellow eye's refractive error was corrected with spectacles, if any. The fellow eye's acuity thus equalled what is reported in columns 8 and 9 of this table. Participants 18 – 30 performed the task with only their spectacles.*